Fluorination-induced half-metallicity in zigzag boron nitride nanoribbons: First-principles calculations

Yanli Wang,[1,*] Yi Ding,[2,3] and Jun Ni[2]

[1]*Department of Physics, Center for Optoelectronics Materials and Devices, Zhejiang Sci-Tech University, Xiasha College Park, Hangzhou, Zhejiang 310018, People's Republic of China*

[2]*Department of Physics, Key Laboratory of Atomic and Molecular Nanoscience (Ministry of Education), Tsinghua University, Beijing 100084, People's Republic of China*

[3]*Department of Physics, Hangzhou Normal University, Hangzhou, Zhejiang 310036, People's Republic of China*

(Received 5 December 2009; revised manuscript received 27 April 2010; published 19 May 2010)

Using first-principles calculations, we investigate the fluorination effect on zigzag boron nitride nanoribbons (ZBNNRs). We find that the fluorination is a practical route to induce half-metallicity in ZBNNRs. When the boron edge is two-fluorine terminated and the nitrogen edge is one-fluorine terminated, the ZBNNRs are stable and become robust half metals regardless of the ribbon width. Our studies demonstrate that these fluorinated ZBNNRs have 100% spin transport polarization around the Fermi level, which leads to promising applications in spintronics and nanodevices.

DOI: 10.1103/PhysRevB.81.193407 PACS number(s): 61.46.−w, 73.22.−f, 73.63.−b

Two-dimensional hexagonal boron nitride (BN) sheets have been successfully synthesized by the micromechanical cleavage technique and chemical-solution-derived method.[1,2] In the high-resolution transmission electron microscopy experiment, vacancies with zigzag edges in BN sheets have been observed,[3] which are confirmed by the latest theoretical work.[4] Two-dimensional hexagonal BN sheet is a wide band-gap semiconductor.[5] The corresponding boron nitride nanoribbons are also semiconductors.[6–8] Due to Coulomb repulsions, the bare nitrogen zigzag edge is spin polarized and leads to half-metallicity in half-passivated zigzag boron nitride nanoribbons (ZBNNRs).[9–12] In our previous work, the stabilities of ZBNNRs with different hydrogen-terminated edges have been determined.[13] We find the bare nitrogen zigzag edge always has a higher energy than the bare boron one in the half-passivated situation.[13] Thus, it is important to find another route to induce half-metallicity in boron nitride nanoribbons.

Fluorine atoms are normally introduced as a chemical functionalization dopant in nanostructures. For the graphene sheet, the fluorination modifies the energy band gap.[14,15] In the zigzag graphene nanoribbons, the fluorinated carbon edges have magnetic edge states.[16,17] For the boron nitride nanostructures, the F-doped BN nanotubes have been synthesized in the experiments.[18] In the BN nanotubes, fluorine atoms prefer to bond with boron atoms rather than nitrogen atoms.[19,20] Recently, it has been reported that the fluorination induces magnetism and can tune ferromagnetic (FM) spin ordering in the BN nanotubes.[21,22] Therefore, it is possible to take the fluorination as an edge-functionalized strategy on boron nitride nanoribbons. In this Brief Report, we use first-principles calculations to investigate the fluorination effect on zigzag boron nitride nanoribbons.

The total energies and electronic structures are calculated by the SIESTA code.[23] In our calculations, we use a double-ζ basis set with additional orbitals of polarization. The local-density approximation (LDA) is adopted for the exchange-correlation (XC) functional and the Troullier-Martins scheme is used for the norm-conserving pseudopotentials. A grid cut-off of 150 Ry is used and the Brillouin-zone samplings are done using $1\times1\times32$ Monkhorst-Pack grids for ZBNNRs. Supercells are used to simulate the isolated nanoribbons and the distance between them is larger than 12 Å. All the structures are relaxed until the maximum atomic force is smaller than 0.04 eV/Å. The transport properties are calculated using the nonequilibrium Green's-function method as implemented in the TRANSIESTA code, which is included in the version 3.0 of SIESTA code.[24]

Since the fluorine gas is supremely reactive, all the dangling bonds at the edges will be passivated and the bare edges are not present. Following the naming convention of hydrogenated ZBNNRs,[13] different fluorinated ZBNNRs are described as BxNy-F types. Here, x (y) takes the values of 1 and 2, which represents the number of fluorine atoms bonding with edge boron (nitrogen) atoms.

Figure 1(a) shows the structure of B1N1-F type, which uses 10-ZBNNRs as a representation. The B1N1-F type of 10-ZBNNRs are semiconductors with an indirect band gap of 4.08 eV while the corresponding hydrogenated B1N1-H type of 10-ZBNNRs have a smaller band gap of 3.84 eV, as shown in Figs. 1(b) and 1(c). The B1N1-F type of nanoribbons is nonmagnetic. The lengths of B-F bonds and N-F bonds are 1.31 Å and 1.37 Å, respectively. In order to determine the stability of the fluorinated nanoribbon from the hydrogenated one, we compare the energies of $E_{FNRs}+\frac{n_H}{2}E_{H_2}$ and $E_{HNRs}+\frac{n_F}{2}E_{F_2}$. E_{FNRs} and E_{HNRs} are the total energies of fluorinated and hydrogenated nanoribbons, and E_{F_2} and E_{H_2} are the total energies of fluorine and hydrogen molecules, respectively. n_H (n_F) is the number of hydrogen (fluorine) atoms doped in nanoribbons, which is equal to $x+y$ for the BxNy type in one unit cell. We obtain the energy difference of the B1N1 type is $E_{FNRs}+E_{H_2}-(E_{HNRs}+E_{F_2})=-4.32$ eV/unit, which indicates that the fluorinated ZBNNRs are stable and can be produced by the fluorination of the corresponding hydrogenated ones. It should be noticed that the fully polar surfaces usually have higher energies than reconstructed or defective polar ones.[25,26] However, for the fluorinated ZBNNRs, we believe the fluorinated zigzag

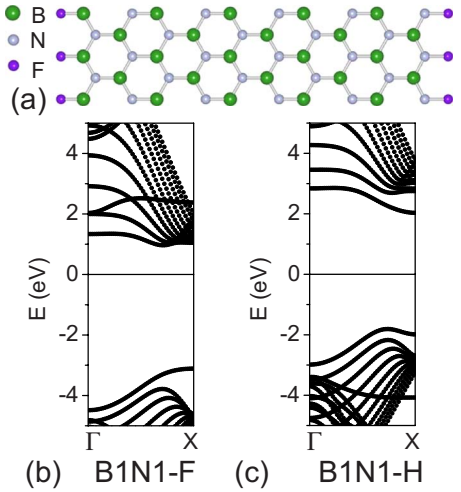

FIG. 1. (Color online) (a) The structure of the B1N1-F type. [(b) and (c)] The band structures of the B1N1-F and B1N1-H type, which are both nonmagnetic.

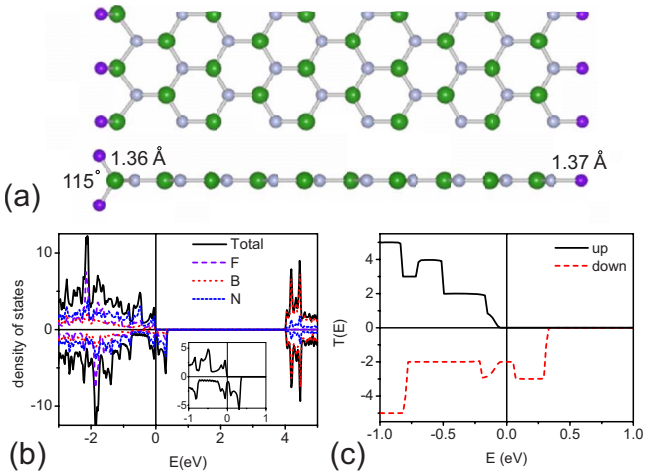

FIG. 2. (Color online) (a) The structure, (b) DOSs, and (c) transmission functions (in G_0, $G_0=e^2/h$) of the B2N1-F type.

edges could exist due to following reasons: (1) in the experiments, the zigzag edges have been observed for large vacancies in the BN sheet.[3] (2) The fluorine atoms bonding to edges can decrease the polarization of nanoribbons. Our calculations find that the B1N1-F type of 10-ZBNNRs has a dipole of 0.27 D/unit, which is smaller than that (2.14 D/unit) of the B1N1-H type. (3) We have constructed a less polar nanoribbons by exchanging a pair of BN atoms in the edge for every two units. Although this system has B-F and N-F bonds in the both edges, it is 0.206 eV/atom higher in energy than that of the B1N1-F type.

Similar to the hydrogenated nanoribbons,[13] we find the B2N1-F type of 10-ZBNNRs are more favorable by −1.76 eV/unit than the B1N2-F type. Thus, we focus the studies on the B2N1-F type of ZBNNRs, which are shown in Fig. 2(a). In this type of structures, the boron edge is two-fluorine terminated and the nitrogen edge is one-fluorine terminated. The local structure of the boron edge is different from the single-fluorinated one. The B-F bonds increase to 1.36 Å and the angle of F-B-F bonds is 115°. We calculate the energy difference as $E_{FNRs}+\frac{3}{2}E_{H_2}-(E_{HNRs}+\frac{3}{2}E_{F_2})=-7.25$ eV/unit. This suggests that the fluorination is strong and the B2N1-F type is stable.

For the B2N1-F type of 10-ZBNNRs, we construct a double unit cell along the nanoribbons to determine the magnetic ground state. The ferromagnetic state is found the most stable. Total energy of the ferromagnetic state is 106 meV/(edge atom) lower than the nonmagnetic state and 41 meV/(edge atom) lower than then the antiferromagnetic (AFM) state. Since these energy differences are larger than the thermal energy k_BT at room temperature (~25 meV), the B2N1-F type of 10-ZBNNRs will maintain the ferromagnetic state above room temperature.

Accompanying with the stable ferromagnetic state, the B2N1-F type of 10-ZBNNRs exhibit half-metallic behaviors. As shown in Fig. 2(b), the spin-up state opens a band gap of 4.08 eV and the top valence band lies below the Fermi level by 0.07 eV. While the spin-down state has densities up to 0.33 eV above the Fermi level. The other n-ZBNNRs of different widths ($n=2-18$) are also calculated. When $n\geq 2$, for all the calculated n-ZBNNRs, the B2N1-F type exhibits half-metallic behavior. Figure 2(c) plots the transmission functions for the spin-up and spin-down channels. The spin transport polarization ξ, which is defined as $\xi=|(T_{up}-T_{down})/(T_{up}+T_{down})|$, is used to measure the spin filtering behavior. In the range of $(-0.07, 0.33)$ eV, the spin-up channel has zero transmittance and the B2N1-F type has $\xi=100\%$ spin transport polarization. Thus, a good spin filter is formed in these fluorinated ZBNNRs.

Previous researches find that half-metallicity of the bare nitrogen edge depends on the XC functional.[9,10] Thus, we need to check the half-metallicity of the B2N1-F type with different XC functionals. Two generalized gradients approximation (GGA) functionals as Perdew-Burke-Ernzerhof (PBE) and Perdew-Burke-Ernzerhof for solids (PBEsol) are used in the calculations. The band structures with different XC functionals are plotted in Figs. 3(a)–3(c). The curve shapes of LDA, PBE, and PBEsol bands are similar to each other. The main influence of the XC functionals is on the energy range in which the spin-up state is insulating and the spin-down state is metallic. It follows the sequence of LDA > PBEsol > PBE. For all the used XC functionals, we obtain the B2N1-F type is a half metal. Thus, the fluorination-induced half-metallicity is robust for the calculations, regardless of LDA and GGA XC functionals.

Figures 3(d) and 3(f) show the module of wave functions $|\psi|$ for the bands crossing the Fermi level. We can see the α and β bands are localized on the two-fluorine-terminated boron edge. The F p_x orbitals and N p_z orbitals make up the α band. The β band is composed of the F p_y orbitals and BN σ bonding orbitals. The two-fluorine-terminated boron edge obtains more electrons than the one-fluorine-terminated one. It induces a large polarization of 4.49 D/unit for the B2N1-F type. The polarization causes a high potential for the electrons at the boron edge.[7] Thus, the top valence bands have the wave functions localized at the boron edge as shown in Fig. 3. Using the difference between the ionization potential and electron affinity of the atoms, we estimate the bare on site Coulomb repulsion of elements.[27] The values are 8.0 eV

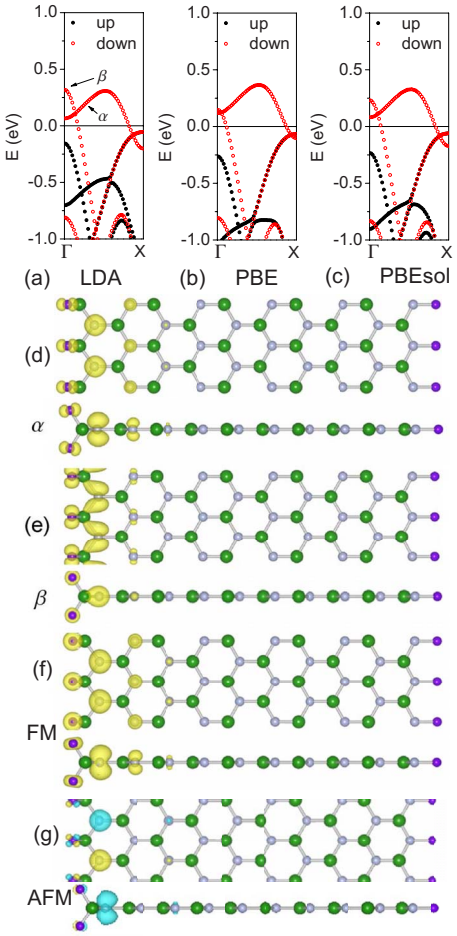

FIG. 3. (Color online) [(a)–(c)] The band structures of the B2N1-F type with different XC functionals. [(d) and (e)] The $|\psi|$ of α and β bands at the Γ point. The isosurface is 25% of the maximum. The spin-density distribution of the B2N1-F type at (f) the FM state and (g) the AFM state. The isosurface is 0.05 $\mu_B/\text{Å}^3$.

for boron, 14.8 eV for nitrogen, and 14.0 eV for fluorine.[28] The large differences between boron and nitrogen/fluorine atoms hinder the charge transfer in the boron edge. Thus, the electrons are localized in the N p and F p orbitals. These orbitals compose the α and β bands as shown in Figs. 3(d) and 3(e), which are spin polarized and lead to half-metallicity. This mechanism is similar to the half-metallic origination of the bare nitrogen edge.[12] For the bare nitrogen edge, it needs electrons localized in the dangling bonds. In the B2N1 type, it requires strong ability of atoms to obtain electrons. Therefore, the hydrogenated B2N1 type of ZBNNRs are not half metals[13] while the fluorinated ones become half metals. Figure 3(f) plots the spin-density distribution of the B2N1-F type. Only the atoms in the boron edge are spin polarized, which is consistent with the above explanation and the partial densities of states (DOSs) in Fig. 2(b).

Finally, we study the properties of the B2N2-F type. Compared with the one-fluorine-terminated nitrogen edge, the local structure of the nitrogen edge in the B2N2-F type is changed. The N-F bonds increase to 1.47 Å and the angle of F-N-F bonds is 95°. The B2N2-F type of 10-ZBNNRs is ferromagnetic metals as shown in Fig. 4(a). We obtain

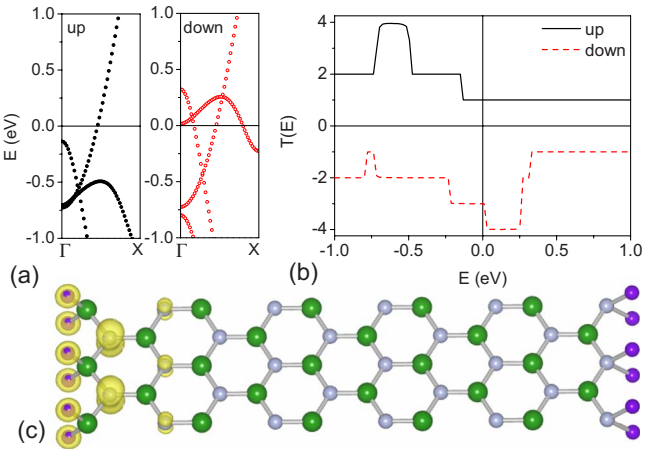

FIG. 4. (Color online) (a) The band structures, (b) transmission functions, and (c) spin-density distribution of the B2N2-F type. The isosurface is 0.1 $\mu_B/\text{Å}^3$.

$E_{FNRs}+2E_{H_2}-(E_{HNRs}+2E_{F_2})=-9.50$ eV/unit. Figure 4(b) shows the B2N2-F type can get $\xi=60\%$ spin transport polarization between (0.03, 0.25) eV. We can see that the two-fluorine-terminated boron edge remains ferromagnetic while two-fluorine-terminated nitrogen edge becomes nonmagnetic as shown in Fig. 4(c), which is the same situation as the hydrogenated B2N2 type.[13]

The stabilities of fluorinated nanoribbons can be determined by the Gibbs free energy $G=\varepsilon_{FNRs}-n_F\mu_F$. Here μ_F is the chemical potential of fluorine and n_F is the number of fluorine atoms. ε_{FNRs} is the formation energy of fluorinated nanoribbons, which is defined as $\varepsilon_{FNRs}=E_{FNRs}-n_{BN}E_{BN\ sheet}-n_F/2E_{F_2}$. n_{BN} is the number of BN pairs, $E_{BN\ sheet}$ is the total energy of the BN sheet per pair, and E_{F_2} is the total energy of fluorine molecules. Thus, for a given value of μ_F, the stable structure has the lowest value of G. Figure 5 shows that the half-metallic fluorinated nanoribbons, B2N1-F type, are stable when the chemical potential is between $(-1.60, 0.12)$ eV. Below -1.60 eV, the single-fluorinated B1N1-F type is stable. Above 0.12 eV, the

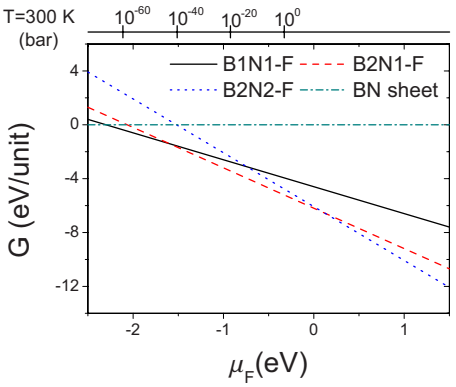

FIG. 5. (Color online) The Gibbs free energies G versus chemical potential of fluorine μ_F for fluorinated nanoribbons. The alternative top axis shows the pressure, in bar, of fluorine gas (molecular F_2) corresponding to the chemical potentials at $T=300$ K (Ref. 29).

double-fluorinated B2N2-F type is stable.

In summary, we have investigated the fluorinated effect on ZBNNRs. The fluorinated ZBNNRs are stable and can be produced by the fluorination of the corresponding hydrogenated ones. We find the ZBNNRs, which have two-fluorine-terminated boron edge and one-fluorine-terminated nitrogen edge, are half metals. Both LDA and GGA calculations confirm the half-metallicity in the fluorinated ZBNNRs. These nanoribbons have 100% spin transport polarization in an energy range of 0.4 eV around the Fermi level and exhibit well spin filtering behaviors. Due to the promising properties, the fluorinated ZBNNRs have potential applications in spintronics and nanodevices.

J.N. acknowledges the support from the National Science Foundation of China (Grant No. 10974107).

*Author to whom correspondence should be addressed; wangyanli-04@tsinghua.org.cn

[1] D. Pacilé, J. C. Meyer, Ç. Ö. Girit, and A. Zettl, Appl. Phys. Lett. **92**, 133107 (2008).
[2] W.-Q. Han, L. Wu, Y. Zhu, K. Watanabe, and T. Taniguchi, Appl. Phys. Lett. **93**, 223103 (2008).
[3] C. Jin, F. Lin, K. Suenaga, and S. Iijima, Phys. Rev. Lett. **102**, 195505 (2009).
[4] S. Okada, Phys. Rev. B **80**, 161404(R) (2009).
[5] M. Topsakal, E. Aktürk, and S. Ciraci, Phys. Rev. B **79**, 115442 (2009); Y. Wang, Phys. Status Solidi (RRL) **4**, 34 (2010).
[6] Z. Zhang and W. Guo, Phys. Rev. B **77**, 075403 (2008).
[7] C.-H. Park and S. G. Louie, Nano Lett. **8**, 2200 (2008).
[8] W. Chen, Y. Li, G. Yu, Z. Zhou, and Z. Chen, J. Chem. Theory Comput. **5**, 3088 (2009).
[9] F. Zheng, G. Zhou, Z. Liu, J. Wu, W. Duan, B.-L. Gu, and S. B. Zhang, Phys. Rev. B **78**, 205415 (2008).
[10] L. Lai, J. Lu, L. Wang, G. Luo, J. Zhou, R. Qin, Z. Gao, and W. Mei, J. Phys. Chem. C **113**, 2273 (2009).
[11] V. Barone and J. E. Peralta, Nano Lett. **8**, 2210 (2008).
[12] F. Zheng, K. Sasaki, R. Saito, W. Duan, and B.-L. Gu, J. Phys. Soc. Jpn. **78**, 074713 (2009).
[13] Y. Ding, Y. Wang, and J. Ni, Appl. Phys. Lett. **94**, 233107 (2009).
[14] N. Lu, Z. Li, and J. Yang, J. Phys. Chem. C **113**, 16741 (2009).
[15] J. Zhou, M. M. Wu, X. Zhou, and Q. Sun, Appl. Phys. Lett. **95**, 103108 (2009).
[16] M. Maruyama and K. Kusakabe, J. Phys. Soc. Jpn. **73**, 656 (2004).
[17] K. N. Kudin, ACS Nano **2**, 516 (2008).
[18] C. Tang, Y. Bando, Y. Huang, S. Yue, C. Gu, F. Xu, and D. Golberg, J. Am. Chem. Soc. **127**, 6552 (2005).
[19] Z. Zhou, J. Zhao, Z. Chen, and P. R. Schleyer, J. Phys. Chem. B **110**, 25678 (2006).
[20] L. Lai, W. Song, J. Lu, Z. Gao, S. Nagase, M. Ni, W. N. Mei, J. Liu, D. Yu, and H. Ye, J. Phys. Chem. B **110**, 14092 (2006).
[21] F. Li, Z. Zhu, X. Yao, G. Lu, M. Zhao, Y. Xia, and Y. Chen, Appl. Phys. Lett. **92**, 102515 (2008).
[22] Z. Zhang and W. Guo, J. Am. Chem. Soc. **131**, 6874 (2009).
[23] J. M. Soler, E. Artacho, J. D. Gale, A. García, J. Junquera, P. Ordejo, and D. Sánchez-Portal, J. Phys.: Condens. Matter **14**, 2745 (2002).
[24] M. Brandbyge, J.-L. Mozos, P. Ordejón, J. Taylor, and K. Stokbro, Phys. Rev. B **65**, 165401 (2002).
[25] J. Goniakowski, F. Finocchi, and C. Noguera, Rep. Prog. Phys. **71**, 016501 (2008).
[26] C. Fang, M. A. van Huis, D. Vanmaekelbergh, and H. W. Zandbergen, ACS Nano **4**, 211 (2010).
[27] S. Dutta, A. K. Manna, and S. K. Pati, Phys. Rev. Lett. **102**, 096601 (2009).
[28] The data of ionization potential and electron affinity is adopted from http://chemed.chem.purdue.edu/genchem/topicreview/bp/ch7/ie_ea.html
[29] The formula of the chemical potential for fluorine is adopted from T. Wassmann, A. P. Seitsonen, A. M. Saitta, M. Lazzeri and F. Mauri, Phys. Rev. Lett. **101**, 096402 (2008); and the data are obtained from D. R. Lide, *CRC Handbook of Chemistry and Physics* (CRC, Boca Raton, 2008).